

University of New Mexico

UNM Digital Repository

Pathology Research and Scholarship

Pathology

7-1-2022

A phenotypic screen for compounds that reverse cAMP-mediated suppression of T cell functions

David Barrett

Department of Molecular and Cell Biology, University of Connecticut, Storrs, CT, United States

Meghan Wyatt

Department of Molecular and Cell Biology, University of Connecticut, Storrs, CT, United States

Haim Bar

Department of Statistics, University of Connecticut, Storrs, CT, United States

Mark K. Haynes

University of New Mexico Center for Molecular Discovery and Department of Pathology, University of New Mexico Health Sciences Center, Albuquerque, NM, United States

Bruce S. Edwards

University of New Mexico Center for Molecular Discovery and Department of Pathology, University of New Mexico Health Sciences Center, Albuquerque, NM, United States

See next page for additional authors

Follow this and additional works at: https://digitalrepository.unm.edu/hsc_path_pubs

Recommended Citation

Barrett D, Wyatt M, Bar H, Haynes MK, Edwards BS, Sklar LA, Zweifach A. A phenotypic screen for compounds that reverse cAMP-mediated suppression of T cell functions. *SLAS Discov.* 2022 Jul;27(5):314-322. doi: 10.1016/j.slasd.2022.03.008. Epub 2022 Apr 3. PMID: 35385793.

This Article is brought to you for free and open access by the Pathology at UNM Digital Repository. It has been accepted for inclusion in Pathology Research and Scholarship by an authorized administrator of UNM Digital Repository. For more information, please contact disc@unm.edu.

Authors

David Barrett, Meghan Wyatt, Haim Bar, Mark K. Haynes, Bruce S. Edwards, Larry A. Sklar, and Adam Zweifach



Full Length Article

A phenotypic screen for compounds that reverse cAMP-mediated suppression of T cell functions

David Barrett^{a,1}, Meghan Wyatt^{a,1}, Haim Bar^b, Mark K. Haynes^c, Bruce S. Edwards^c, Larry A. Sklar^c, Adam Zweifach^{a,*}

^a Department of Molecular and Cell Biology, University of Connecticut, Storrs, CT, United States

^b Department of Statistics, University of Connecticut, Storrs, CT, United States

^c University of New Mexico Center for Molecular Discovery and Department of Pathology, University of New Mexico Health Sciences Center, Albuquerque, NM, United States

ARTICLE INFO

Keywords:

Cancer
Tumor microenvironment
Immunity
Cell signaling

ABSTRACT

The solid tumor microenvironment (TME) suppresses immune responses. Three alterations in the TME converge on a pathway triggered by elevated cyclic AMP (cAMP) that suppresses T cell receptor (TCR) signaling. We developed a phenotypic assay to screen for small molecules that interfere with this pathway using TALL-104 human leukemic cytotoxic T lymphocytes pretreated with prostaglandin E2 to elevate cAMP. Beads coated with anti-CD3 antibodies stimulate lytic granule exocytosis, which is detected via binding of an antibody against lysosome associated membrane protein 1 (LAMP-1) measured with flow cytometry. Confirming that the assay can find compounds with desired activity, treating cells with a phorbol ester restores exocytosis. The assay behaves well in 96-well format and we screened a collection of compounds expected to have effects on epigenetic regulatory proteins. Compounds in this collection affected lytic granule exocytosis after 24-hour treatment, but none prevented cAMP from suppressing lytic granule exocytosis. We used a fully automated 384-well version of the assay to screen the Prestwick Compound Library but obtained no confirmed hits. Analyzing this assay's performance reveals two points of interest. First, cytometry offers multiple ways to quantify signals. Z' was higher using percent positive cells than mean fluorescence because the relationship between the two measures saturates, but using percent positive could make it harder to find hits in some assays. Second, variance was higher in positive controls than in negative controls in this assay, which degrades assay performance less than if variance was higher in negative controls.

Introduction

Solid tumors create an environment that suppresses anti-tumor immune responses (see [1,2] for reviews). Overcoming this will be vital for future advances in cancer treatments. Three major immune-suppressing factors generated in the tumor environment- PGE₂ [3], adenosine [4,5] and tumor associated regulatory T cells (T_{regs}) [6,7] act at least in part by increasing intracellular cAMP in effector T (T_{eff}) and natural killer (NK) cells, triggering an intracellular signaling cascade that suppresses their tumoricidal activity. PGE₂ is produced as a result of COX2 activity upregulated in multiple cell types, including tumor cells themselves, fibroblasts, epithelial cells and infiltrating lymphocytes, including T_{regs}⁸. Extracellular ATP released into the tumor milieu is converted to adenosine by CD39 and CD73, which are expressed together or singly on tumor cells, fibroblasts, and T cells, including T_{regs}, and mesenchymal stem

cells [4,9] T_{regs} are present in the tumor microenvironment in large numbers as a result of chemokines, cytokines and PGE₂ [6,7]. PGE₂ and adenosine can then activate EP2 and EP4 or A2 G-protein coupled receptors, respectively, stimulating adenylyl cyclase (AC) in T_{eff} cells, while T_{regs} can directly transfer cAMP into the cytoplasm of T_{eff} cells via gap junctions [6]. Each of the steps described represents a point of intervention that could be exploited to block immunosuppression [5,7,8]. A problem, though, is that blocking any one of them would spare the others, so function would still be suppressed.

Once elevated in T_{eff} cells, cAMP activates cAMP-dependent protein kinase (PKA), which in turn phosphorylates and activates csk, a tyrosine kinase with homology to src-dependent protein kinases (Wehbi and Taskén, 2016). Csk binds to a number of scaffold proteins that reside in lipid rafts in a complex and dynamic fashion. Upon phosphorylation by PKA, csk interactions with scaffolds are weakened, and it

* Corresponding author.

E-mail address: adam.zweifach@uconn.edu (A. Zweifach).

¹ These authors contributed equally.

binds to and phosphorylates the src-family tyrosine kinase lck, inactivating it and thus inhibiting signaling mediated by T cell receptors (TCRs). Unlike interventions aimed at the upstream pathways, blocking this effector cell-intrinsic pathway offers the possibility of disabling the three upstream pathways at a common point. Results in cells expressing genetically-engineered csk mutants that can be inhibited with 3-iodo-PP1 [11] demonstrate desired downstream effects of ablating this pathway pharmacologically. This provides support for the idea that targeting it with small molecules could produce useful phenotypic effects. Unfortunately, the components identified to date are not attractive drug targets. Efforts to develop selective small molecule inhibitors of PKA and AC have so far not been notably successful, and blocking them would likely have a wide range of effects on heart, brain and kidneys (see e.g. [12]). Csk is very similar in sequence and structure to src kinases, so it is unlikely that small molecule csk inhibitors could be developed that do also not block T cell activation.

Here, we describe a screen for compounds that prevent cAMP-mediated immunosuppression. The screen is based on TALL-104 leukemic human T cells [13] and high throughput flow cytometry (HTFC) [14,15], a system we have used for several previous screens for immunomodulatory small molecules [16,17]. We measure lytic granule exocytosis, which is stimulated by polystyrene beads coated with anti-CD3 antibodies mimicking activation through the TCR, by detecting binding of a fluorescently-labeled antibody against the lysosomal protein CD107a/ LAMP-1. We treat cells so as to elevate cAMP, suppressing responses through the TCR and then screen for compounds that restore responses. We believe that, since the proteins known to be involved are unlikely to be good drug targets, this assay might be a good way to identify compounds that work by currently-unknown mechanism.

Materials and methods

Cells and reagents- TALL-104 cells were from the ATCC and grown as described previously [16]. TCS, Bw5147 cells stably transfected with an anti-CD3 sc-FV [24], were a gift of Dr. Peter Steinberger (Medical University of Vienna). Prostaglandin E2 was from Sigma. Phorbol 12-myristate 13-acetate (PMA) was from Alexis Biochemical. Thapsigargin (TG) was from adipoGEN. Anti-LAMP antibody Alexa Fluor 647 conjugate was purchased in bulk from: Biolegend. CD3 and CD8 Dynabeads, Calcein red-orange AM, Celltrace CFSE, and DAPI were from Thermo Fisher. The collection of compounds purported to alter epigenetic regulation (Item #: 11,076_0446183) was from Cayman Chemical and was a gift from Dr. Charles Giardina, UConn Department of Molecular and Cell Biology.

Flow cytometry for detection of lytic granule exocytosis and 96-well screening of the epigenetic compound library- Flow cytometry was used to measure exocytosis in TALL-104 cells. All experiments were performed on a BD Fortessa X20 equipped with an autosampler at the University of Connecticut's COR2E Flow Cytometry Facility and analyzed using FlowJo Software (version 9 or 10). To assess effects of agents that elevate cAMP, cells were plated at a density of 2×10^6 /ml in complete medium and pretreated with 10 μ M prostaglandin E2, forskolin, 8-B-cAMP (all in DMSO) or vehicle alone for 30 min at 37C, then stimulated by adding anti-CD3 coated Dynabeads together with anti-LAMP antibody. Cells were incubated for two hours at room temperature with rotation prior to acquisition. Anti-CD8 coated Dynabeads were used as a negative control.

A set of 80 compounds (plate 1) from the Cayman Chemical Epigenetic screening library was screened for activity in three assays. 1) To test for effects on TCR-independent lytic granule exocytosis, TALL-104 cells were plated in 100 μ L at a density of 2×10^6 /mL with 1 μ L 10 mM compound at a final concentration of 10 μ M and incubated at 37C for 24 h in a CO2 incubator. Cells were stimulated with TG and PMA at final concentrations of 1 μ M and 50 nM, respectively, in the presence of anti-LAMP antibody and were incubated for 2 h. 2) To test for effects on TCR-dependent lytic granule exocytosis, TALL-104 cells

were plated in 100 μ L at a density of 2×10^6 / ml with compounds at a final concentration of 10 μ M and incubated at 37C for 1 hour then stimulated by adding solution containing anti-CD3 coated Dynabeads, and anti-LAMP antibody for two hours at room temperature with rotation. Anti-CD8 coated Dynabeads were used as a negative control. 3) To test for prevention/ reversal of PGE2-mediated immunosuppression, TALL-104 cells were pretreated with 10 μ M prostaglandin E2 for 30 min at 37C prior to treatment as in (2) above.

Simultaneous measurement of target cell killing and granule exocytosis- TALL-104 cells were incubated in culture media with calcein red-orange AM at a final concentration of 1 μ M for 10 min and then washed. They were then treated with DMSO, PGE2, or PMA for 30 min. TCS cells were washed and resuspended in PBS at a cell concentration of 2×10^6 cells/ml containing Celltrace CFSE at 1 μ L/ ml. After 20 min, the dye was quenched with media and the cells were washed and resuspended. Cells were then mixed and co-incubated for a total of 3 h. Each sample contained 5×10^4 TCS in 200 μ L, with TALL-104 cells added to achieve the desired effector to target ratio. After two hours, labeled anti-LAMP antibody was added to the solution, and DAPI was added 45 min later. To test the ability of PMA to restore responses, 50 nM PMA was added when the cocultivation started, and the effector to target: ratio was 1:1.

384-well screening of the Prestwick Compound Library- Translating this assay to 384-well plates required using two plates: an assay plate and a reagent plate. A diagram outlining the assay is shown in Fig. 1. Assay plates were created first. Compounds were delivered by acoustic dispensing (LabCyte Echo 555; 20 nL of 10 mM stock) from library plates that were stored frozen. Then, 10 μ L of assay medium was added to columns 1 and 2 using a BioTek dispenser, and 10 μ L of complete medium +20 μ M PGE2 was added to columns 3–23. Column 24 served as a wash column and received 20 μ L of complete medium. Plates were then mixed for 1 min at 1200 RPM. Ficoll-purified TALL-104 cells were resuspended to 2×10^6 /ml in complete medium. Then, using the BioTek dispenser, cells were added to columns 1–23 (5 μ L/well at a starting density of 2×10^6 /ml) resulting in a final concentration of 10,000 cells/well. Reagent plates were created while cells were incubating with compounds and PGE2. The required volume of anti-CD3 or anti-CD8 Dynabeads was washed twice with buffer (3 min, 2500 RPM using normal Ringers). Once beads were washed, they were resuspended to 4.8×10^6 /ml in normal Ringer's that also contained a 1/80 dilution of Alexa Fluor 647-labeled anti-LAMP-1 antibody stock and dispensed using the BioTek dispenser. For the 4 plate test of the Prestwick Chemical Library, the reagent plate contained 16 μ L of beads with 2 μ L excess left as dead volume. An Agilent Biocel was then used to transfer 4 μ L from wells of the reagent plate to each assay plate well to mix beads and antibody with dispensed cells. The final assay wells contained 10,000 cells at 0.5×10^6 /ml, compounds at a final concentration of 12.5 μ M, PGE2 at a final concentration of 13.3 μ M and total DMSO at ~0.12%. Covered plates were incubated and protected from light for 4 h at 20 C. Assay wells were sampled with a Gilson peristaltic pump and GX274 sampler. Approximately 1.5 μ L was collected from each well. This resulted in acquisition (from Plate 1 of the run) of 2415 +/- 1033 (mean +/- SD) total events, of which 1029 +/- 455 were single cells bound to a single bead. Data were acquired with either a Beckman Coulter Cyan Adap or BD Accuri cytometer as a single file that was then parsed into the corresponding 368 sampled wells using HyperSip and HyperView software, which identifies individual sample wells, tabulates cytometric data, and merges chemical library files with cytometer-derived fluorescence values.

Analysis of assay performance- Assay performance was simulated essentially as described previously [18] using R software [19]. R.app GUI 1.77 (7985 High Sierra build) was used. For these simulations, the compound collection was assumed to contain 200,000 compounds. 99,900 were completely inactive, 100,000 were exponentially distributed from no activity to completely active (activity = 100), and two additional compounds (100 total) were added to each activity level bin from 51

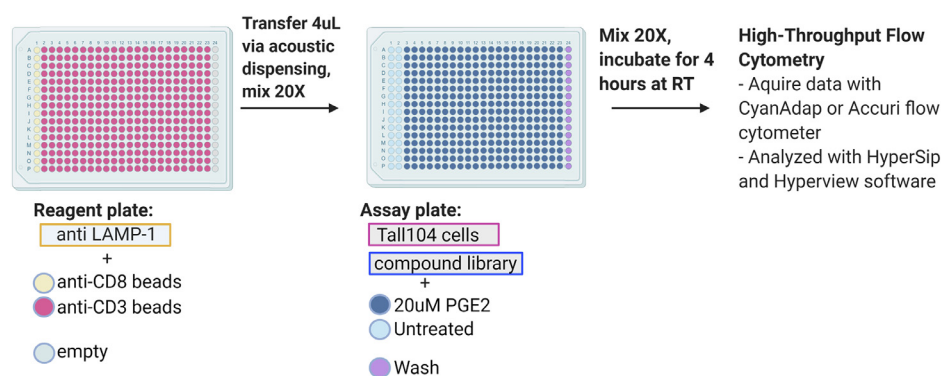


Fig. 1. Schematic illustrating HTS of Prestwick compound library in 384-well plates. The reagent plate contains LAMP1 antibody as well as anti-CD3 and anti-CD8 beads. This plate is transferred to the assay plate, which contains TALL-104 cells treated or untreated with PGE2, and the compound library. The final assay plate is incubated for 4 h at RT before analyzed using high-throughput flow cytometry. This figure was created with Biorender.com.

to 100. 788 virtual compounds had activity > 50%. Simulations were averaged 10 times to smooth the results.

Results

Increasing cAMP inhibits TCR-stimulated lytic granule exocytosis in TALL-104 human leukemic CTLs- TALL-104 cells release lytic granules in response to beads coated with anti-CD3 antibodies, which can be detected by increased binding to cells of fluorescently-labeled antibodies against LAMP-1/ CD107a [20]. We reasoned that if responses were to be inhibited by treatments that elevate cAMP, this could serve as the basis for a phenotypic screen for compounds that reverse cAMP-mediated immunosuppression. We tested the effects of several agents expected to elevate cAMP, including the membrane permeant cAMP analog 8-Br-cAMP [21], forskolin [22] and prostaglandin E2 (PGE2) [23], on exocytosis. All substantially reduced responses (Fig. 2A). PGE2 produced the most robust suppression, which we thought would be important for obtaining well-separated responses in screening. The two relevant PGE2 receptor isoforms expressed on lymphocytes are the prostanoid receptors EP2 and EP4, and we detected expression of both proteins in TALL-104 cells using immunocytochemistry (Fig. 2B). We confirmed that treating TALL-104 cells with PGE2 results in elevated intracellular cAMP using a luminescence-based detection kit (Supplemental Figure 1). Consistent with the effects on exocytosis, the increase in cAMP stimulated by PGE2 was larger than that triggered by forskolin. Immunoblotting could have provided additional evidence for EP2/ EP4 receptors. However, since 1) PGE2's only known actions are mediated by cAMP, 2) PGE2 potently elevates cAMP in TALL-104 cells and 3) PGE2 and two other cAMP elevating treatments all inhibit lytic granule exocytosis, we believe that there is sufficient evidence to support using PGE2 as the most robust means of elevating cAMP for further experiments. To confirm that effects on lytic granule exocytosis are due to downregulation of TCR signaling rather than effects on lytic granule exocytosis itself, we assessed the effects of PGE2 on responses stimulated by the combination of TG+PMA, soluble chemicals that act downstream of the TCR to trigger granule exocytosis. Exocytosis was only affected by treatment of cells with PGE2 at treatment times of at least 24 h (data not shown), consistent with the that inhibition of TCR stimulated responses seen after 30 min pretreatment is due to suppression of TCR signaling.

To test whether effects detected via decreases in anti-LAMP-1 antibody binding are physiologically relevant, we measured effects on target cell killing and granule exocytosis simultaneously (Fig. 2C). We used a murine thymoma that has been engineered to express a single-chain anti-CD3 (scFv anti-CD3), referred to as T cell stimulators (TCS) [24], as target cells in these experiments. TCS should bind to TALL-104 cells and stimulate lytic granule exocytosis like anti-CD3 coated beads. We labeled TCS with the amine-reactive dye CFSE so that membrane permeabilization due to perforin pore formation would not result in dye loss, and we labeled TALL-104 cells with calcein red-orange. After incubation for four hours we added DAPI as a means of identifying target

cells with compromised membrane integrity, along with anti-LAMP-1 antibody to allow measurement of TALL-104 granule exocytosis. To analyze responses, a very broad scatter gate was first applied to exclude the many small particles that are present after coincubation of the two cell types, as the large number of these particles (which likely represent debris) would compromise attempts to quantify the percentage of target cells that have been killed. We then applied gates based on CFSE and calcein red-orange fluorescence to identify TCS and TALL-104 cells, computed the percentage of DAPI-positive TCS to estimate target cell killing, and computed the percentage of anti-LAMP positive TALL-104 cells as a measure of lytic granule exocytosis. In the absence of TALL-104 cells, ~10% of TCS were DAPI+ after incubation, likely reflecting baseline cell death. Adding increasing numbers of TALL-104 cells results in an increasing percentage of DAPI+ TCS. At effector: target ratios of only 2.5:1 ~90% of TCS were DAPI+. Furthermore, the TALL-104 cells that were coincubated with TCS were stained with anti-LAMP-1 antibody, as expected. When TALL-104 cells were pretreated with PGE2 for 30 min and then coincubated with TCS in the continued presence of PGE2, killing was reduced by ~50% and staining of TALL-104 cells with anti-LAMP antibody was also reduced. TALL-104 cells can also use NK receptors to trigger lytic granule exocytosis and kill NK sensitive targets such as K562 cells, which PGE2 suppresses as well (data not shown). We wanted to be certain that killing of TCS was due to the targeting scFv anti-CD3 acting via TCRs. We coincubated cells in the presence of an excess of soluble anti-CD3, which we reasoned would compete with the scFv anti-CD3. Both killing and granule exocytosis were substantially reduced in the presence of soluble anti-CD3.

As mentioned above, we view the best use of this assay as screening for compounds that work by unknown mechanism rather than by inhibiting any of the proteins we already know to be involved (EP2/EP4, AC, PKA, etc.), as these are unlikely to be suitable targets due to their broad expression and involvement in multiple fundamental processes. To make sure that restoring responses in PGE2-treated cells is possible, we reasoned that PMA, which does not cause exocytosis in TALL-104 cells on its own, might synergize with residual signaling through the TCR as was shown to be the case for ingenol, another PKC-activating compound, in T cell exhaustion [25]. We first tested this idea using anti CD3-bead stimulation. In four independent experiments, we observed a near-doubling of responses from the PGE2- suppressed level when cells were also treated with PMA (data not shown). We then examined PMA's effects using our method for monitoring killing and exocytosis at the same time (data for lytic granule exocytosis are shown in Fig. 2D). Although PGE2-inhibited lytic granule exocytosis was enhanced by PMA as expected based on the results with anti-CD3 beads, target cell killing was not restored (data not shown).

An assay for compounds that prevent cAMP-mediated immunosuppression- Building on the results described above, we designed a straightforward 96-well plate assay for compounds that prevent cAMP-stimulated downregulation of T cell activation. We add PGE2 to DMSO- or compound-treated TALL-104 cells to elevate

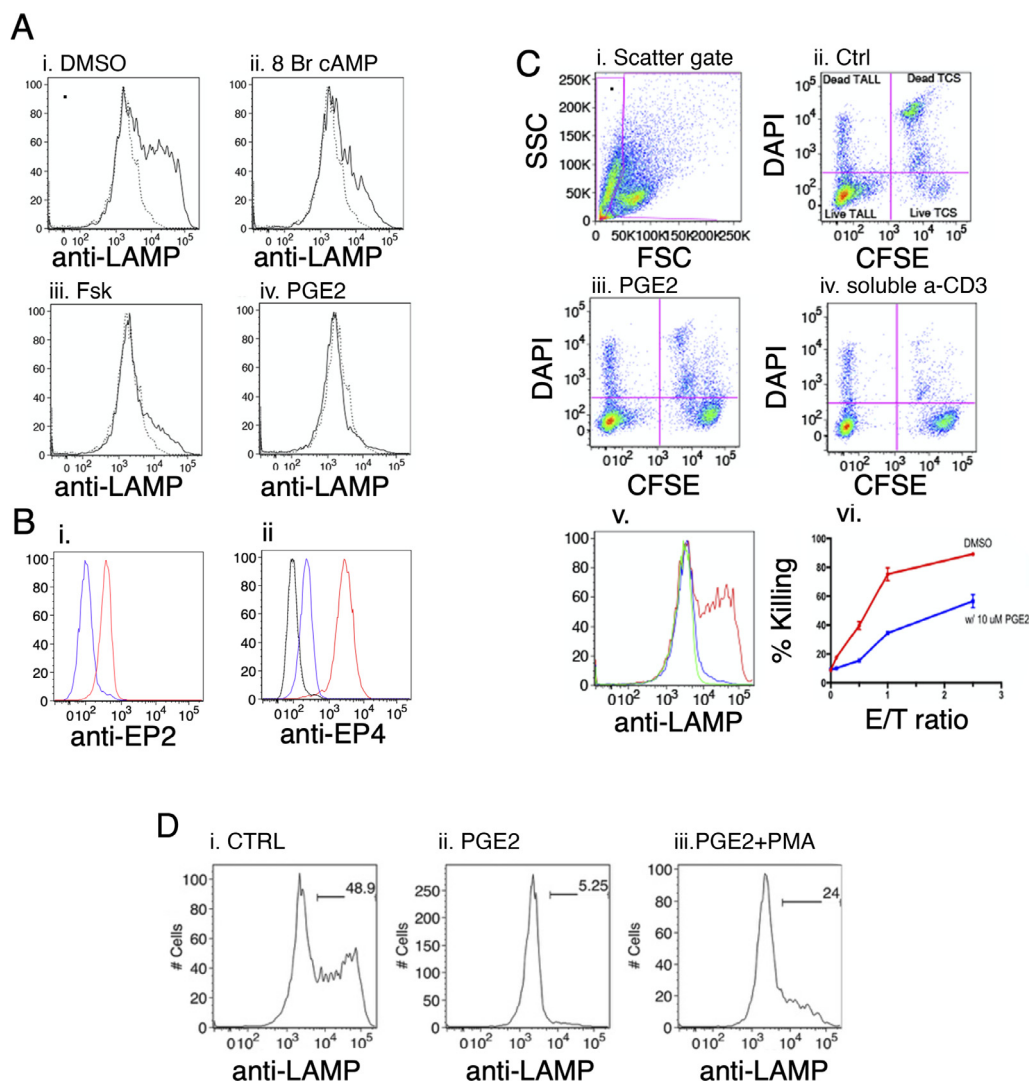


Fig. 2. PGE2 suppresses lytic granule exocytosis and target cell killing in TALL-104 human leukemic CTLs. A) Lytic granule exocytosis in cells bound to anti-CD3 beads is inhibited by elevating cAMP. Histograms of anti-LAMP-1 staining for cells bound to beads coated with anti-CD8 (dashed lines) or anti-CD3 (solid lines) are shown for cells pretreated as indicated. B) TALL-104 cells express EP2 and EP4 receptors. (i) Cells were stained with a fluorescently-labeled anti-EP2 monoclonal antibody (red) or not stained (blue). (ii) Cells were incubated with an anti-EP4 antibody followed by a fluorescent secondary antibody (red), stained with the secondary antibody alone (blue), or left unstained (green). C) Target cell killing is inhibited by PGE2. i) Plot of FS vs. SSC showing the gate that was used to exclude very small debris. ii-iv) Plots of DAPI vs. CFSE fluorescence when TALL-104 cells (CFSE-) were incubated with TCS (CFSE+) at an effector: target ratio of 2.5:1 under the conditions indicated. v) Histograms of anti-LAMP fluorescence from the CFSE- populations (TALL-104 cells) shown in ii (red), iii (blue) and iv (green). vi) Percent target cell killing calculated from data like that shown in ii-iv at different effector: target ratios in the presence of DMSO (red) or 10 μ M PGE2 (blue). D) Histograms of anti-LAMP fluorescence from TALL-104 cells that were treated with and without PGE2 or PMA, mixed with TCS as in Fig. 2C.

cAMP, then stimulate them by adding anti-CD3 beads. We then select cells bound to a single bead by gating on scatter and fluorescence, and quantify signals using one of two metrics that are available in flow cytometry. The first is simply the geometric mean fluorescence intensity of the cells. The second is the percentage of positive cells, measured by setting a threshold on an unstimulated sample and then applying that threshold to determine the relative number of cells with fluorescence exceeding that value. To test whether our assay is robust enough for screening, we first laid out 96-well plates with alternating columns of DMSO- and PGE2- treated cells (Table 1). In this experiment, DMSO serves as the positive control, generating a high signal, while PGE2 (dissolved in DMSO) serves as a negative control, giving a low signal. Z' was routinely > 0.5 when either measure was used to quantify lytic granule exocytosis indicating, based on the criteria originally defined by Zhang et al., that the assay is in

the category considered “excellent” [26]. We next screened a set of compounds selected for putative effects on epigenetic regulatory mechanisms, hoping that after 24-hour treatment they might produce changes in global protein networks that could weaken or inactivate the response to cAMP, generating an increase in the anti-LAMP signal in PGE2-treated samples. To confirm that these compounds have relevant biological activities, we tested their effects in two other assays using TALL-104 cells. In the first, cells were stimulated with the soluble chemicals TG+PMA, which act downstream of the TCR (Fig. 3A, B), while in the second, cells were stimulated with anti-CD3 beads but not pretreated with PGE2 (Fig. 3C). In both assays, numerous compounds inhibited responses. Notably, when signals measured using percent positive were plotted against geometric mean fluorescence intensity, pronounced saturation behavior was evident in the assay conducted with TG+PMA. As a result, compounds that inhibited substantially

Table 1
Performance of the Assay in 96-well Format.

	Negative Control		Positive Control		Z'	
	G.M.	% Pos	G.M.	% Pos	G.M.	% Pos
Plate 1	2687 (183)	15.3 (2.0)	14,383 (1802)	62 (4)	0.49	0.61
Plate 2	2022 (124)	5.2 (0.8)	7813 (757)	30 (2.4)	0.54	0.61
Plate 3	2726 (143)	2.3 (0.3)	12,085 (1277)	58 (3.7)	0.54	0.78

Values are the mean and SD (in parenthesis) of 41 and 42 values for negative and positive controls, respectively, for Plate 1, and 48 values for both controls for the other plates.

The phosphodiesterase inhibitor IBMX (0.5 mM) was used with PGE2 in Plate 3.

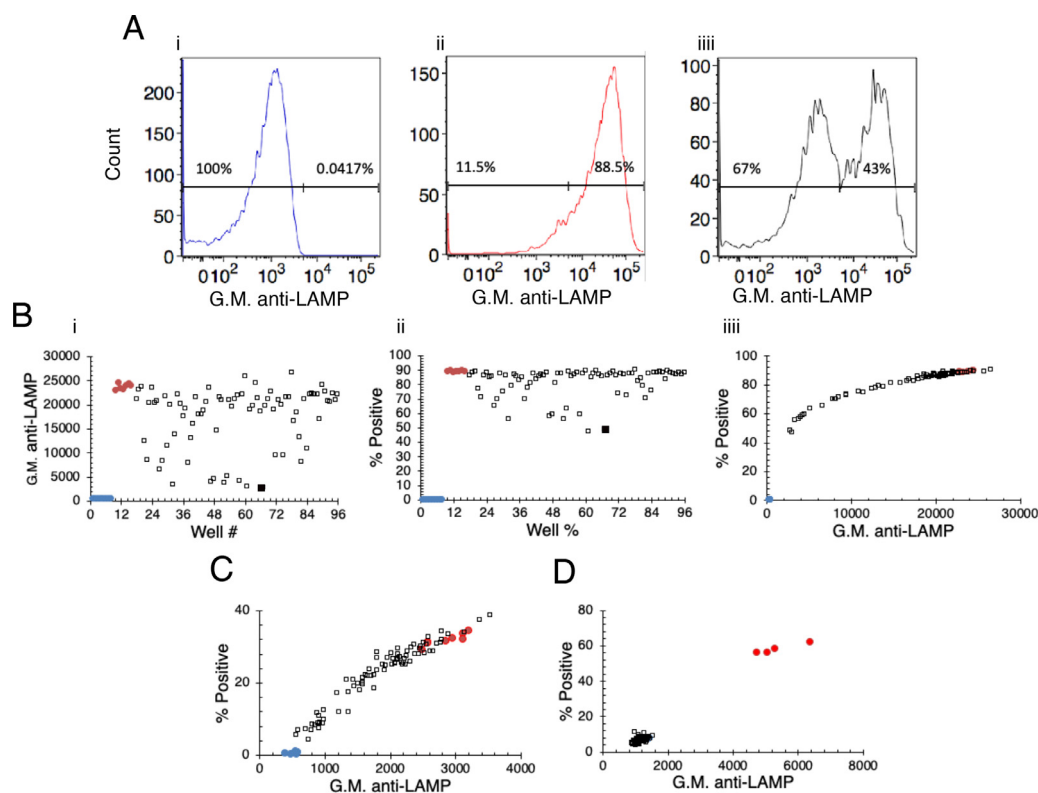


Fig. 3. Screening a collection of compounds that affect epigenetic regulators in 96-well plates. A) Histograms of anti-LAMP fluorescence for i) unstimulated cells, ii) cells stimulated with TG+PMA and iii) stimulated cells treated with one of the compounds from the epigenetic regulator set. Gates used to set thresholds for computing percent positive cells are shown, with the percentage of cells that responded indicated. B) Plots of data from the experiment shown in (A) analyzed by i) computing the geometric mean fluorescence intensity or ii) computing the percent positive cells. The two measures are plotted against each other in (iii). Blue circles are DMSO-treated positive controls, red circles are TG+PMA stimulated negative controls and open squares are compound-treated cells, except the compound-containing well shown in A, which is represented by a filled square. C) Plot of percent positive cells vs. geometric mean fluorescence for cells incubated with the epigenetic regulator set then stimulated with anti-CD3 beads. Data are displayed as described for (B). D) As in C, except cells were treated with PGE2 after incubation with the epigenetic regulator compounds.

when measured using geometric mean appeared to be considerably less effective when measured using percent positive. Unfortunately, none of the compounds tested reversed the effects of PGE2 treatment on lytic granule exocytosis (Fig. 3D), although we note that compounds that substantially inhibited responses stimulated by anti-CD3 beads might not be able to restore PGE2-inhibited responses even if they did interfere with cAMP's actions. The pronounced inhibitory effects of compounds in this set on lytic granule exocytosis might be interesting to investigate further.

A 384-well format of the assay- We next developed a 384-well format of the assay using entirely automated cell and reagent handling and used it to screen the Prestwick Compound Library (Fig. 4). We were able to perform a single successful run of the Prestwick Compound Li-

brary, which we analyzed to gain insights into assay performance. When we analyzed data by computing the geometric mean of the anti-LAMP fluorescence intensity, after excluding outliers Z' for the four plates was 0.3, 0.5, 0.0 and 0.4. If all points were included Z' computed over all four plates was 0, which has come to be generally regarded as inadequate to proceed with screening- in the terminology defined by Zhang et al. This would be a "yes-no" assay. Using percent positive to quantify fluorescence improved the apparent performance of the assay- the four plates had Z' of 0.7, 0.8, 0.6 and 0.6, and Z' computed over the four plates was 0.6 when all points were included. Plotting data for the four plates using the two measures against each other shows why this is the case. As expected from the results in Fig. 3, the relationship between the two measures saturates at high signal levels. This means that variance rela-

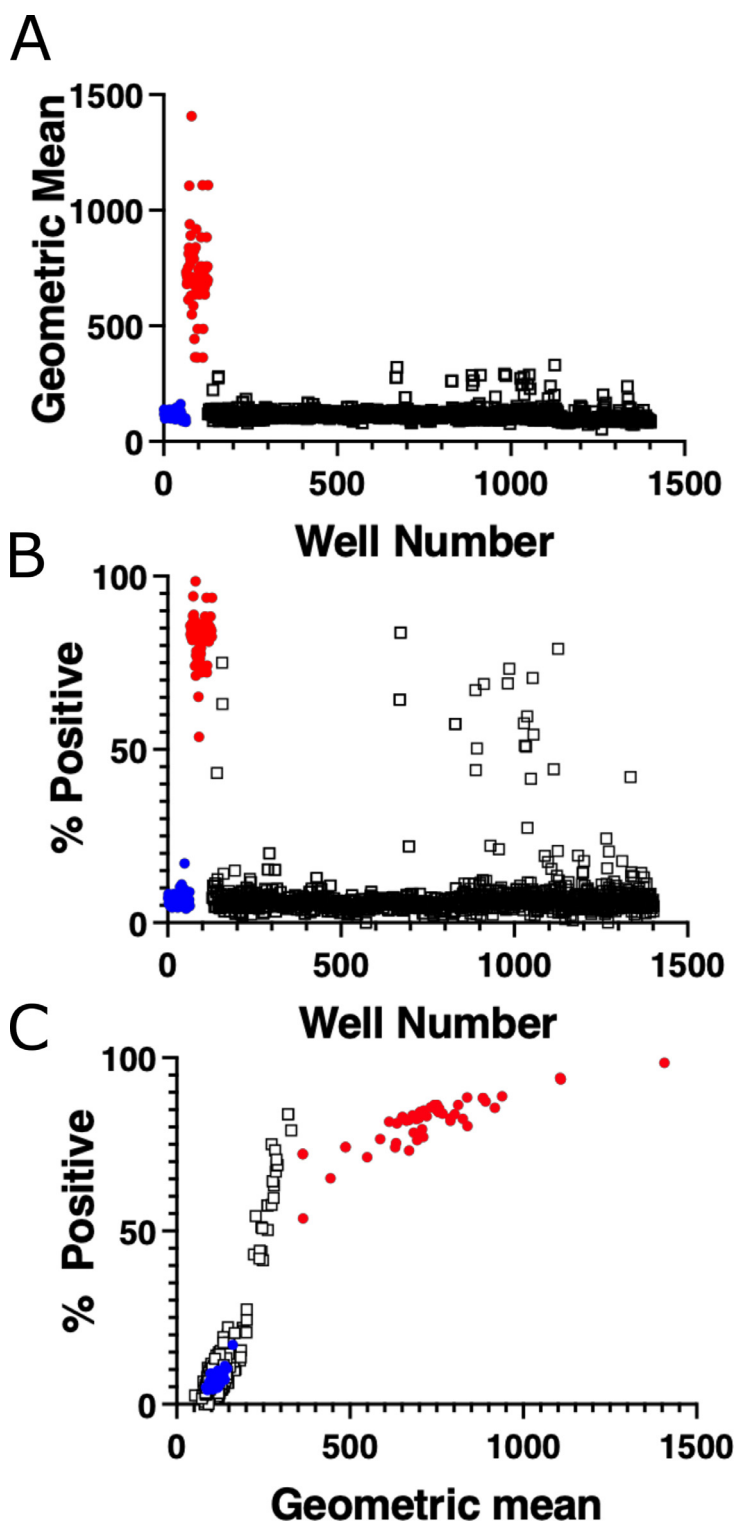


Fig. 4. Screening the Prestwick Compound Library in 384-well plates. A) Data from the four plates of the collection analyzed by calculating geometric mean fluorescence intensity. Blue circles are the PGE2-treated negative controls, red circles are the DMSO-treated positive controls and open squares are the compound-treated samples. B) Same as in (A), except the data were analyzed by setting a threshold and computing percent positive cells. C) Plot of the data from (A) against the data in (B).

tive to signal amplitude in the positive control population is lower using percent positive compared to when geometric mean is used and since Z' is directly proportional to variance the result is that Z' is lower. Several compounds that appeared to enhance PGE2-stimulated responses were found in this single screen of PCL, but as of yet we have not had the opportunity to retest them to confirm their activity. Based on our previous experience with this collection, many are likely fluorescent artifacts generating spurious actives.

In the current assay, variance is higher for positive controls than negative controls, which is opposite to cases we previously simulated [18] (and likely also opposite to the case in most assays for inhibitors). This makes a big difference to assay performance. We recently developed a simulation approach to assessing assay performance [18], and we have applied it to the 384-well version of the assay (Fig. 5). For these simulations, we assumed a slightly different underlying library composition than in our previous work. The simulated collection here contains

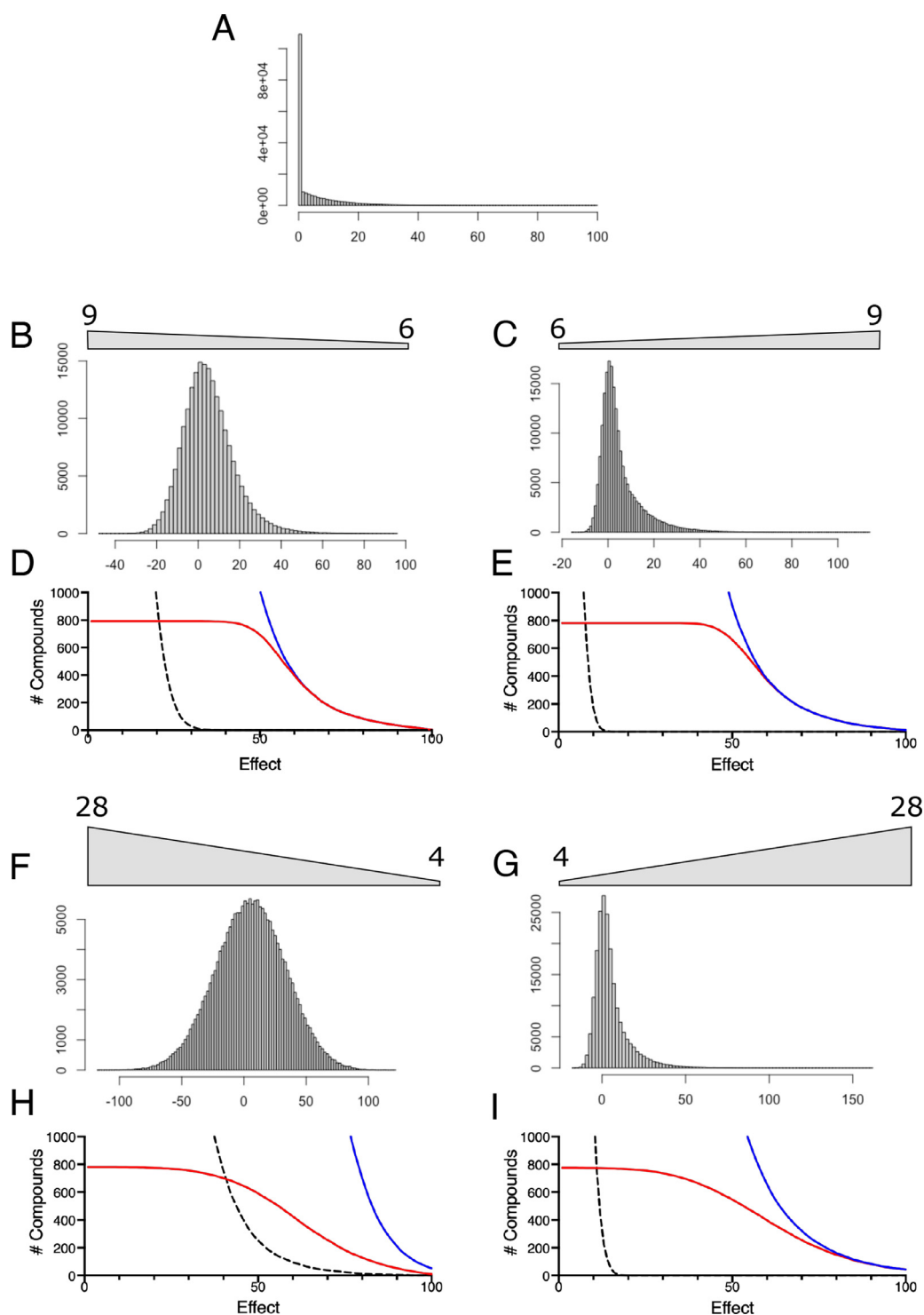


Fig. 5. Analyzing the performance of the 384-well assay. A) Histogram of the assumed actual distribution of activity in the compound collection. B) Histogram of the apparent distribution of activity when SD in the inactive compounds is 9 and decreases linearly to a value of 3 for the most active compounds as indicated above the plots in this and subsequent panels. C) Histogram of apparent activity when SD is 3 in the inactive compounds and increases linearly to 9 for the most active. D) Plots of the total number of compounds found (blue), the number of compounds that really inhibit >50% found (red) and the number of totally inactive compounds found (black dotted) as a function of apparent activity for the data in (B). E) as in (D), but for the data in (C). F) Histogram of apparent activity when SD is 28 for the inactive compounds and decreases linearly to 4 for the most active. G) Histogram of apparent activity when SD is 4 for the inactive compounds and increases linearly to 28 for the most active. H) As in (D) for the data in (F). As in (D) for the data in (G).

200,000 compounds. 99,900 are completely inactive (i.e. have zero effect). 100,000 are exponentially distributed from 0 effect to completely (100%) effective. Finally, 2 compounds have been added to each effect level bin between 51 and 100. The total number of compounds >50% effective in the collection was 788. Using the Z' values and distributions of noise observed in the 384-well version of our assay reveals the following. Using percent positive as the metric, the assay has a Z' of ~ 0.6 . Whether noise is higher in the positive controls (as it is in this assay) or in the negative controls, performance is similar. For both, if a threshold of $\sim 50\%$ effect is chosen, ~ 1000 compounds will be selected as active, and ~ 700 of those should really inhibit by 50% or more. However, when Z' is 0, as it is if geometric mean fluorescence is used to quantify signals, the way in which variance changes becomes very important. An assay in which variance is higher in the negative control population will find 1000 apparently active compounds at a threshold of $\sim 80\%$, but only 200 of those will really be $>50\%$ active. At thresholds $<80\%$, increasing numbers of completely inactive compounds tend to be misidentified as active. In contrast, when $Z' = 0$ and variance is higher in the positive control population, the assay behaves reasonably well, and does a good job of finding compounds. If a threshold of $\sim 55\%$ effect is chosen, 1000 compounds will be selected, and almost 600 of them will in reality be $>50\%$ effective.

Discussion

We have previously developed several assays based on TALL-104 lytic granule exocytosis, including a multiple treatment-time assay in which TALL-104 cells bar-coded with calcein-AM and treated with compounds for different times were stimulated with anti-CD3 beads [16]. The assay reported here was the most difficult to adapt to fully automated 384-well format because of the multiple combinations of different beads (anti-CD3 and anti-CD8) and the need to add PGE2 to some but not all wells. We solved this by creating a separate reagent plate from which aliquots of beads and antibody could be transferred to assay plates (see Fig. 1). One limitation of this approach is that cells are exposed to compound and PGE2 at the same time, which may not be optimal as pretreatment with compound prior to exposure to PGE2 might be more likely to abrogate immunosuppression. Including treatment with compounds prior to PGE2 would complicate the assay since it is necessary to preincubate cells with PGE2 before adding anti-CD3 beads to allow time for suppression, but this could likely be solved if necessary. Our assay is in some ways similar to that of Marro et al. [25], who generated exhaustion in transgenic mouse CTLs by infecting them with lymphocytic choriomeningitis virus (LCMV) and then screened for compounds that restored expression of YFP driven by an IFN- γ promoter- in both cases, a phenotypic state of interest related to the tumor microenvironment was induced in cells in order to then screen for inhibitors.

As mentioned, we believe the best use of this assay would be to try to identify compounds that interfere with cell-intrinsic pathways of cAMP-mediated immunosuppression by currently-unknown mechanism, since the molecules already known to participate are not particularly attractive drug targets. To do so, it would be necessary to identify and exclude hits that work by blocking known targets- EP2/ EP4, *Gas*, adenylyl cyclase, and PKA- so that these can be excluded. It is possible to test effects on each of these individually, but the quickest approach might be to measure effects on substrate phosphorylation by PKA using antibodies specific for phosphorylated PKA substrates, since inhibition of any one of the components listed would block PKA activity in response to PGE2. Hits could interfere with currently-unknown components of the pathway, including interactions that localize csk to rafts [27] and/or AKAPs that anchor PKA [10] (Fig. 6). Protein-protein interactions are difficult targets, but there have been some notable successes [28]. Alternatively, hits could enhance residual signaling that persists after lck downregulation, as was found recently to be the case for the PKC-activating com-

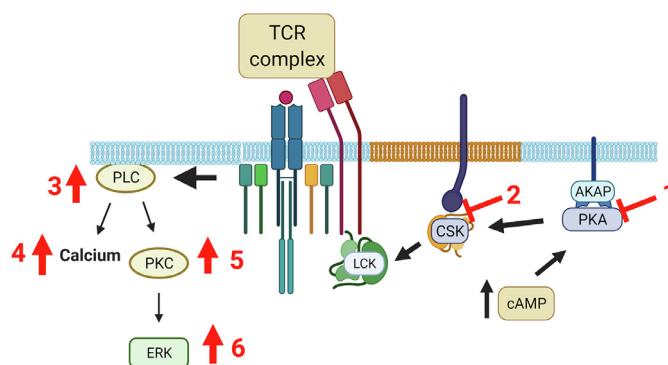


Fig. 6. Overview of potential mechanisms of hit compounds. Disruption of cAMP mediated immune suppression can occur through action on a number of targets proximal to TCR signaling that are impacted by elevated cAMP. Compounds could reduce signals upstream of the TCR via (1) disruption of PKA membrane anchoring or (2) disruption of CSK raft localization (raft lipids are indicated in orange). Compounds could also act downstream of the TCR to enhance (3) activity of PLC, (4) calcium signaling, (5) activity of PKC, or (6) activity of ERK. This figure was created with Biorender.com.

pound ingenol in a model of T cell exhaustion [25] and as we showed for PMA in TCR-stimulated lytic granule exocytosis. In our hands, PMA did not restore target cell killing, likely because its actions are not correctly spatially localized to the point of contact with the target where an immunological synapse is known to form. Hits that restore exocytosis but do not enhance target cell killing may still be of some use provided they restore other T cell functions like cytokine production that are also suppressed by cAMP in the tumor microenvironment.

We previously investigated the significance of the commonly-used assay metric Z' , concluding that it did not provide a particularly useful descriptor of assay performance [18]. Our examination of the performance of the 384-well version of our assay reinforces the notion that assay development should not simply be a matter of seeking to maximize Z' . First, there are multiple ways to quantify signals in flow cytometry. Computing the percentage of positive cells can yield higher Z' than measuring mean fluorescence intensity because of the saturating relationship between the two measures. This effect is not unique to this assay, we have also observed it in other antibody-binding assays and in assays based on fluorescent protein expression (data not shown). While it might seem that since a measure like the percentage of positive cells cannot be normally distributed it would be improper to use it to compute Z' , there is in fact no real statistical grounding for Z' so this is not a problem. However, the percentage of positive cells should not be the default way of analyzing flow cytometry screening data even though it can yield lower Z' . In a screen for enhancement like this one the range in which signals are of interest occurs on a linear portion of the relationship between percentage of positive cells and geometric mean so it is on balance advantageous to use percent positive. However, in a screen for inhibitors, apparent activity could be substantially reduced for weaker hits if the percentage of positive cells rather than the geometric mean is used (see Fig. 3A-C) which might cause those hits to be missed. Therefore, the choice between geometric mean and percent positive should be made after careful consideration of the controls and how a possible distribution of compounds of interest would appear relative to those controls. Second, the results reinforce something we noted before: assays can have the same Z' but behave very differently depending on how noise is distributed. Based on considerations like these, researchers should put less emphasis on “optimizing” assays by simply maximizing Z' . Our simulation approach shows that basic considerations of the properties of an assay can greatly alter how the assay performs at finding compounds of interest. We hope tools like our simulation approach can help make this kind of analysis routine.

Declaration of Competing Interest

Adam Zweifach reports financial support was provided by National Institutes of Health. Larry Sklar reports financial support was provided by National Institutes of Health.

Acknowledgements

This work was supported by NIH grant [AI121069](#) to AZ, and by NIH grants [UL1TR001449](#) and [P30CA118100](#) to LAS. We would like to acknowledge the outstanding assistance by Dr. Wu He of the University of Connecticut's COR2E Flow Cytometry Facility.

Supplementary materials

Supplementary material associated with this article can be found, in the online version, at doi:[10.1016/j.slasd.2022.03.008](#).

References

- [1] Arina A, Corrales L, Bronte V. Enhancing T cell therapy by overcoming the immunosuppressive tumor microenvironment. *Semin Immunol* 2016;28:54–63. doi:[10.1016/j.smim.2016.01.002](#).
- [2] Spranger S, Gajewski TF. Mechanisms of tumor cell–intrinsic immune evasion. *Ann Rev Cancer Biol* 2018;2(1):213–28. doi:[10.1146/annurev-cancer-bio-030617-050606](#).
- [3] Brudvik KW, Taskén K. Modulation of T cell immune functions by the prostaglandin E2 – cAMP pathway in chronic inflammatory states. *Br J Pharmacol* 2012;166(2):411–19. doi:[10.1111/j.1476-5381.2011.01800.x](#).
- [4] Allard B, Beavis PA, Darcy PK, Stagg J. Immunosuppressive activities of adenosine in cancer. *Curr Op Pharmacol* 2016;29:7–16. doi:[10.1016/j.coph.2016.04.001](#).
- [5] Sek K, Mølck C, Stewart GD, Kats L, Darcy PK, Beavis PA. Targeting Adenosine Receptor Signaling in Cancer Immunotherapy. *Int J Mol Sci* 2018;19(12). doi:[10.3390/ijms19123837](#).
- [6] Klein M, Bopp T. Cyclic AMP Represents a Crucial Component of Treg Cell-Mediated Immune Regulation. *Front Immunol* 2016;7. doi:[10.3389/fimmu.2016.00315](#).
- [7] Ohue Y, Nishikawa H. Regulatory T (Treg) cells in cancer: can Treg cells be a new therapeutic target? *Cancer Sci* 2019;110(7):2080–9. doi:[10.1111/cas.14069](#).
- [8] Liu B, Qu L, Yan S. Cyclooxygenase-2 promotes tumor growth and suppresses tumor immunity. *Cancer Cell Int* 2015;15(1):106. doi:[10.1186/s12935-015-0260-7](#).
- [9] Antonioli L, Blandizzi C, Pacher P, Haskó G. Immunity, inflammation and cancer: a leading role for adenosine. *Nature Rev Cancer* 2013;13(12):842–57. doi:[10.1038/nrc3613](#).
- [10] Wehbi VL, Taskén K. Molecular mechanisms for cAMP-mediated immunoregulation in T cells – role of anchored protein kinase A signaling units. *Front Immunol* 2016;7. doi:[10.3389/fimmu.2016.00222](#).
- [11] Manz BN, Tan YX, Courtney AH, et al. Sakaguchi S, editor Small molecule inhibition of Csk alters affinity recognition by T cells. *Elife* 2015;4:e08088. doi:[10.7554/eLife.08088](#).
- [12] Yan K, Gao LN, Cui YL, Zhang Y, Zhou X. The cyclic AMP signaling pathway: exploring targets for successful drug discovery. *Mol Med Rep* 2016;13(5):3715–23. doi:[10.3892/mmr.2016.5005](#).
- [13] Cesano A, Santoli D. Two unique human leukemic T-cell lines endowed with a stable cytotoxic function and a different spectrum of target reactivity analysis and modulation of their lytic mechanisms. *In Vitro Cell Dev Biol* 1992;28A:648–56.
- [14] Edwards BS, Sklar LA. Flow Cytometry Impact on Early Drug Discovery. *J Biomol Screen* 2015;20(6):689–707. doi:[10.1177/1087057115578273](#).
- [15] Kuckuck FW, Edwards BS, Sklar LA. High throughput flow cytometry. *Cytometry* 2001;44:83–90.
- [16] Zhao Z, Henowitz L, Zweifach A. A multiplexed assay that monitors effects of multiple compound treatment times reveals candidate immune-enhancing compounds. *SLAS Discov* 2018;23:646–55. doi:[10.1177/2472555218777731](#).
- [17] Zhao Z, Haynes MK, Ursu O, Edwards BS, Sklar LA, Zweifach A. A high-throughput phenotypic screen of cytotoxic T lymphocyte lytic granule exocytosis reveals candidate immunosuppressants. *J Biomol Screen* 2015;20:359–72. doi:[10.1177/1087057114557620](#).
- [18] Bar H, Zweifach A. Z' Does Not Need to Be >0.5. *SLAS Discov* 2020;25(9):1000–8. doi:[10.1177/2472555220942764](#).
- [19] Core Team R. R: a Language and Environment for Statistical Computing. R Found Stat Comput 2020. <https://www.R-project.org/>.
- [20] Zhao Z, West AM, Balunas MJ, Zweifach A. Development of an Enhanced Phenotypic Screen of Cytotoxic T-Lymphocyte Lytic Granule Exocytosis Suitable for Use with Synthetic Compound and Natural Product Collections. *J Biomol Screen* 2016;21(6):556–66.
- [21] Tatsukawa Y, Bowolaksono A, Nishimura R, Komiyama J, Acosta TJ, Okuda K. Possible roles of intracellular cyclic AMP, protein kinase C and calcium ion in the apoptotic signaling pathway in bovine luteal cells. *J Reprod Dev* 2006;52(4):517–22. doi:[10.1262/jrd.18024](#).
- [22] De Felici M, Dolci S, Pesce M. Proliferation of mouse primordial germ cells in vitro: a key role for cAMP. *Dev Biol* 1993;157(1):277–80. doi:[10.1006/dbio.1993.1132](#).
- [23] Rincón M, Tugores A, López-Rivas A, et al. Prostaglandin E2 and the increase of intracellular cAMP inhibit the expression of interleukin 2 receptors in human T cells. *Eur J Immunol* 1988;18(11):1791–6. doi:[10.1002/eji.1830181121](#).
- [24] Leitner J, Kuschei W, Grabmeier-Pfistershammer K, et al. T cell stimulator cells, an efficient and versatile cellular system to assess the role of costimulatory ligands in the activation of human T cells. *J Immunol Methods* 2010;362:131–41. doi:[10.1016/j.jim.2010.09.020](#).
- [25] Marro BS, Zak J, Zavareh RB, Tejjaro JR, Lairson LL, Oldstone MBA. Discovery of small molecules for the reversal of T cell exhaustion. *Cell Rep* 2019;29(10):3293–302 e3. doi:[10.1016/j.celrep.2019.10.119](#).
- [26] Zhang JH, Chung TD, Oldenburg KR. A simple statistical parameter for use in evaluation and validation of high throughput screening assays. *J Biomol Screen* 1999;4:67–73.
- [27] Vang T, Abrahamsen H, Myklebust S, Horejsí V, Taskén K. Combined spatial and enzymatic regulation of Csk by cAMP and protein kinase A inhibits T Cell Receptor Signaling. *J Biol Chem* 2003;278(20):17597–600. doi:[10.1074/jbc.C300077200](#).
- [28] Scott DE, Bayly AR, Abell C, Skidmore J. Small molecules, big targets: drug discovery faces the protein–protein interaction challenge. *Nature Rev Drug Discov* 2016;15(8):533–50. doi:[10.1038/nrd.2016.29](#).